Deuterium analysis by inductively coupled plasma mass spectrometry using polyatomic species: an experimental study supported by plasma chemistry modeling

Gábor Galbács, Albert Kéri, Ildikó Kálomista, Éva Kovács-Széles, Igor B. Gornushkin

PII: S0003-2670(20)30013-1

DOI: https://doi.org/10.1016/j.aca.2020.01.011

Reference: ACA 237370

To appear in: *Analytica Chimica Acta*

Received Date: 22 August 2019

Revised Date: 20 November 2019

Accepted Date: 5 January 2020

Please cite this article as: G. Galbács, A. Kéri, I. Kálomista, É. Kovács-Széles, I.B. Gornushkin, Deuterium analysis by inductively coupled plasma mass spectrometry using polyatomic species: an experimental study supported by plasma chemistry modeling, *Analytica Chimica Acta*, https://doi.org/10.1016/j.aca.2020.01.011.

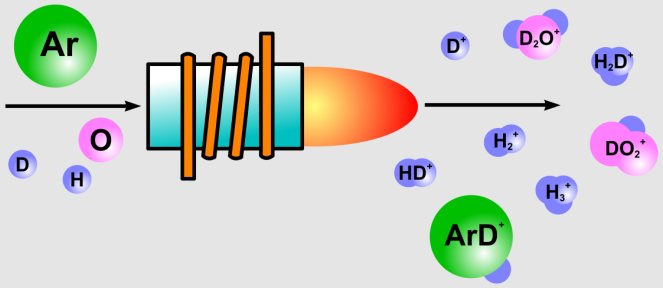

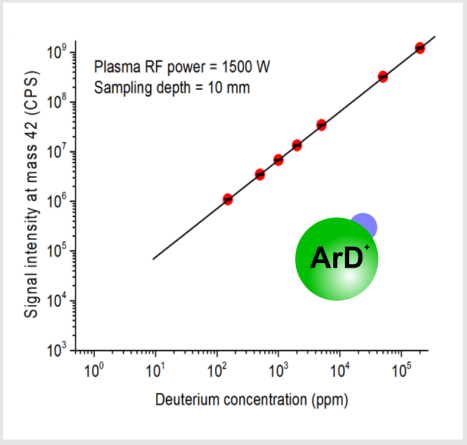

Deuterium analysis by inductively coupled plasma mass spectrometry using polyatomic species: an experimental study supported by plasma chemistry modeling

Gábor Galbács[a*], Albert Kéri[a], Ildikó Kálomista[a], Éva Kovács-Széles[b], Igor B. Gornushkin[c]

[a]Department of Inorganic and Analytical Chemistry, University of Szeged,

Dóm square 7, 6720 Szeged, Hungary

[b]Nuclear Security Department, MTA Centre for Energy Research,

Konkoly Thege Miklós street 29-33, 1121 Budapest, Hungary

[c]BAM Federal Institute for Materials Research and Testing,

Richard-Willstaetter-Strasse 11, 12489 Berlin, Germany

*Corresponding author, e-mail: galbx@chem.u-szeged.hu, tel: +36-62-544013

Abstract

A new analytical method is proposed for the determination of deuterium (D) by ICP-MS. The method is based on the use of the signal from hydrogen-containing polyatomic ions formed in the inductively coupled plasma. Prior to analytical experiments, a theoretical study was performed to assess the concentration of polyatomic species present in an equilibrium Ar-O-D-H plasma, as a function of temperature and stoichiometric composition. It was established that the highest sensitivity and linearity measurement of D concentration in a wide range can be achieved by monitoring the ions of D_2 and ArD, at masses 4 and 42, respectively. Results of the calculations are in good agreement with the experiments. Signal stability, spectral interferences, as well as the effect of plasma parameters were also assessed. Under optimized conditions, the limit of detection (LOD) was found to be 3 ppm atom fraction for deuterium when measured as ArD (in calcium and potassium free water), or 78 ppm when measured as D_2. The achieved LOD values and the 4 to 5 orders of magnitude dynamic range easily allow the measurement of deuterium concentrations at around or above the natural level, up to nearly 100% (or 1 Mio ppm) in a standard quadrupole ICP-MS instrument. An even better performance is expected from the method in high resolution ICP-MS instruments equipped with low dead volume sample introduction systems.

Keywords: deuterium; deuterium-enriched water; deuterium-depleted water; inductively coupled plasma-mass spectrometry; hydrogen; polyatomic species

1. Introduction

Analysis of the isotopic composition of water provides important data for the study of the biological, geological, and chemical processes in the environment. Assessing isotopic fingerprints and understanding sources of isotopic fractionation of water are key to answer scientific questions in biogeochemistry. Hydrogen stable isotope measurements are of particular interest in these fields [1], but they also play important role e.g. in forensic investigations [2] or in tracing the geographical origin of food [3]. Deuterated (heavy) water is also used in certain types of nuclear fission reactors as neutron moderator [4], and in ^{1}H-NMR spectroscopy as solvent, either to eliminate the signal contribution from ^{1}H in regular ("light") water or to identify labile hydrogens in organic molecules [5]. The International Atomic Energy Agency uses analysis of heavy water in nuclear safeguards system to detect undeclared activities in nuclear facilities (e.g. illegal production of plutonium from ^{238}U). Deuterium-depleted water has even been suggested as a new tool in cancer therapy due to its biological effects [6]. All these applications require hydrogen stable isotope analysis.

Depending on the accuracy and sensitivity required, several techniques are available for hydrogen stable isotope analysis of water. The most accurate and most sensitive, well established reference method is isotope ratio mass spectrometry (IRMS), which has been used for decades. The IRMS technique can only analyze gaseous samples, therefore water has to be converted to hydrogen prior to analysis by either reduction with hot metals or via high temperature pyrolysis [7]. Another, more recent, sensitive measurement technique is isotope ratio infrared spectroscopy (IRIS). IRIS laser instrumentation is cheaper and more compact than IRMS, moreover it works with water vapor, so requires almost no sample preparation. However, it was shown to be prone to spectral interferences from organic contaminants, such as alcohols, therefore

its accuracy is inferior to IRMS, except if very careful corrections are applied [8, 9]. Site-specific natural isotope fractionation nuclear magnetic resonance (SNIF-NMR) is another accurate technique extensively used for $^{2}H/^{1}H$ as well as $^{13}C/^{12}C$ isotope ratio analysis, mainly for food provenance analysis. $^{2}H/^{1}H$ analysis was the first and still is the most important application of SNIF-NMR [10]. In addition to the above, several other less sensitive or less accurate analytical techniques have been also proposed or are available commercially for the determination of stable hydrogen isotopes e.g. either in industrial applications or for elucidating synthesis reaction pathways. These techniques include Raman spectroscopy [11], gas chromatography [12], FTIR spectroscopy [13] and laser induced breakdown spectroscopy (LIBS) [14, 15]. Density and refractive index measurements are also in use for e.g. D_2O concentration measurements at the percent level.

Inductively coupled plasma mass spectrometry (ICP-MS) has a well recognized potential for studying the stable and radiogenic isotope ratios in environmental, biomedical, nuclear or cosmochemical studies. The robustness, high ionization efficiency and very low detection limits of the technique are greatly appreciated in many scientific fields. Single collector ICP-MS instruments usually only allows the execution of less demanding isotope ratio measurements with modest precision, whereas the state-of-the-art multicollector (sector-field) ICP-MS instrumentation provides very good precision (0.002% RSD). An excellent overview of the status of isotopic analysis by ICP-MS is provided by the book edited by Vanhaecke and Degryse [16]. Most ICP-MS isotope ratio measurements focus on the determination of isotopes of metals (mainly strontium, lead, uranium, thorium, etc.) and only occasionally of light elements, like Li, B and S [3, 16, 17]. Isotopes of other organogenic, light elements, such as H, C, N, O are generally not available for ICP-MS analysis due to high background

concentrations, spectral interferences and low ionization efficiencies. Space charge effects also strongly affect the measurement of light isotopes, even in sector-field ICP-MS instruments, that are normally used for accurate isotope ratio analysis. Determination of hydrogen stable isotopes by ICP-MS in particular is further complicated by *i)* easy exchange of the sample isotopes with the environment facilitated by the usually open autosampler vessels, and *ii)* the useful mass range of several ICP-MS instruments does not cover masses below 4. Due to these reasons, and to the best knowledge of the authors, the determination of hydrogen stable isotopes by ICP-MS in aqueous samples has not been attempted in the literature yet.

The presence of polyatomic ions in the background spectrum of ICP-MS has been detected in the early years already [18, 19]. The most serious analytical problems are caused by those polyatomic species which incorporate elements that are present in the ICP-MS at high concentration, such as Ar, O, N, H, or in cases when the interfered analyte is monoisotopic (e.g. ^{75}As and $^{40}Ar^{35}Cl$). Tables of common polyatomic ions have been compiled and published in the literature several times (e.g. [20, 21]). Identification, formation and dissociation of two or three atomic ions have been investigated over the years by Houk et al. and others using different methodologies, such as accurate mass measurements with high resolution spectrometers, identification by isotope ratios, determination of dissociation temperatures or isotope exchange experiments [22-26]. It has been established that some experimental conditions, such as the material of the sampling cone as well as the ion extraction voltage can influence the intensity of polyatomic ions in the background spectrum, but in general, still little is known about the details of their formation mechanisms. In general, the approach to polyatomic spectral interferences is rather pragmatic in the ICP-MS community; understandably it mainly focuses on their elimination, and much less on their detection or determining

their reaction pathways. Mitigation or elimination of this interference is possible, in the majority of cases, by the application of collision or reaction cell technology [27], preferably in combination with a tandem mass analyzer [28], or a high resolution sector-field instrument [16].

In particular, the literature on deuterium containing polyatomic species is scarce and it also focuses on the elimination of certain interferences. Namely, it was suggested to use D_2O as solvent/diluent instead of H_2O as a means to shift the mass of hydride polyatomic ions thereby freeing certain analyte signals from the interference or to make their identification easier [26]. Smith and Houk [29] successfully used this approach to suppress the signal from $^{36}Ar^{1}H^{+}$ in order to make the determination of $^{35}Cl/^{37}Cl$ possible. A detection limit of about 20 ppb for ^{35}Cl and a 0.21% RSD precision (in a 50 ppm solution of LiCl) for the chlorine isotope ratio was achieved. Zoriy et al. [30] used the same approach to reduce the formation of UH^{+} ions for the purpose of the accurate determination of $^{236}U/^{238}U$ ratios. They compared the performance of several sample introduction systems combined with three sector field ICP-MS instruments and obtained uranium isotope ratio results for certified samples with better than 1.2% RSD precision and around 1% relative accuracy.

The concept we would like to introduce in our present study for the mitigation of some of the problems hindering the analysis of hydrogen stable isotopes by ICP-MS is not to eliminate hydrogen-containing polyatomic species, but on the contrary, to use them as signal proxies for indirect analysis. This can help to shift the mass of analyte to a higher (≥4) mass that is measurable on all instruments and is potentially less interfered, similarly to the mass-shift mode of reaction cell technology. The upward mass shift can also help to increase the sensitivity and reduce matrix effects via partially suppressing space charge effects. Here, we focus on the sensitive quantitative

determination of the concentration of deuterium (D) by considering the polyatomic species containing D. Due to kinetic and stoichiometric reasons, such reactions lead to some sensitivity reduction, thus in order to maintain a reasonable level of sensitivity, high concentration reaction partners should be considered for hydrogen. Therefore, mainly argon and oxygen, as well as hydrogen itself may be considered as a partner. The validity of the concept can be tested involving the following prominent two and three atomic species: DH, D_2, DH_2, OD, OD_2, O_2D, ArD, ArD_2.

The goal of this analytical work was to investigate the feasibility and analytical potential of deuterium determination by ICP-MS based on the use of the signal from hydrogen-containing polyatomic species. This assessment was made by *i)* constructing an equilibrium plasma chemistry model to predict the concentration of suitable polyatomic species in the ICP plasma, also considering thermodynamic stability of the species and *ii)* performing analytical experiments using aqueous solutions with certified deuterium content and monitoring the signal from selected polyatomic species. The influence of experimental parameters on the analytical performance of the method was also assessed in detail.

2. Materials and methods

2.1. Instrumentation

Analytical experiments were carried out using a quadrupole Agilent 7700x ICP-MS (Santa Clara, USA) equipped with standard Agilent I-AS autosampler. The sample introduction system contained a peristaltic pump, a MicroMist microflow concentric pneumatic nebulizer and a Peltier-cooled Scott type spray chamber. The instrumental parameters were set up according to standard conditions: 15.0 L/min plasma gas flow rate, 1.05 L/min carrier gas flow rate, 40 µL/min sample uptake rate. The applied

instrument control software was the Agilent MassHunter provided by the manufacturer. The instrument was capable of measuring m/z values in the 2 – 260 range. During measurements the equipped ORS^3 collision cell of the instrument was turned off to preserve the polyatomic species produced in the plasma.

The evaporation rate for deuterated and regular water was monitored using an Ohaus AP110S (Ohaus Europe, Neanikon, Switzerland) analytical balance.

2.2. Materials

Deuterium-depleted water (with 1 ppm D) and deuterium-enriched (99.96 atom % D) water samples were obtained from Sigma Aldrich (St. Louis, USA). Samples with other deuterium concentrations were prepared by mixing these two certified water samples. In certain experiments trace analytical purity water from a Millipore Elix 10/Synergy UV labwater system (Merck, Darmstadt, Germany), considered to contain the typical 150 ppm atom% D, was also used as sample. For the investigation of spectral interferences hindering deuterium analysis analytical purity $CaCl_2$ (Carl Roth GmbH & Co. KG, Karlsruhe, Germany) and KCl (VWR International, Pennsylvania, USA) salts were commercially obtained.

2.3. Notation and methods

In this work, the approach described in [31-33] is used to model chemical reactions in plasmas. The existence of local thermodynamic equilibrium (LTE) conditions in the plasma were considered. For the processes of ionization, recombination, chemical dissociation, and chemical bonding, the number densities of electrons, atoms, molecules, and atomic and molecular ions are determined by solving the Saha, charge conservation, Guldberg–Waage, and elemental mass conservation equations at given temperature and

pressure. The LTE assumption is generally accepted for ICPs, for example on the basis of the overlap of reported experimental temperature values (translational, excitation, vibrational, and rotational) [34]. As it was noted in [33], the choice of a particular set of reactions is not important in LTE; it is therefore convenient to choose a set, in which every neutral molecule dissociates completely into neutral atoms. The reaction and ionization constants are computed using partition functions of species involved in chemical reactions. The partition functions for molecules and their positive and negative ions are calculated using the latest experimental and ab initio data for spectroscopic constants. The method of calculation of molecular partition functions and other relevant information is given in the Appendix. The multi-reaction equilibrium is solved by a hierarchical algorithm proposed in [33]. Three different subroutines are used for high, medium, and low temperatures: the contraction principle, Newton-Raphson, and scaled Newton-Raphson methods, correspondingly.

For convenience, the following notation was used throughout this paper for the isotopes of hydrogen: H for protium (^{1}H), D for deuterium (^{2}H). Please also note that for the purposes of plasma chemistry modeling only the elements of hydrogen, oxygen and argon, originating from the water sample and the plasma gas, were considered. In addition, only the most abundant isotopes of oxygen and argon, namely ^{40}Ar (99.6003%) and ^{16}O (99.757%), were included in the calculations [35]. For this reason, isotope masses are only indicated if relevant. The same also applies to the charge of the detected species (single positive charge). All deuterium concentrations in the study are meant, unless stated otherwise, as deuterium atom concentrations, that is [D]/[D+H] atom or mole fractions.

All programming was done in Matlab2019a (Mathworks, USA). Graphs were prepared in Origin 8.6 software (OriginLab, USA) and Matlab.

3. Results and discussion

3.1. Modeling of the chemical composition of the plasma

When water, which contains H_2O, HDO and D_2O in various proportions in accordance with the level of deuteration, is nebulized into an argon ICP plasma, the molecules vaporize in the high temperature (~5000 K) argon plasma and undergo thermal dissociation, ionization and recombination. A chemical network will hence consist of atomic hydrogen, oxygen and argon and their most important molecules O_2, H_2, H_3, OH, H_2O, H_2O_2, HO_2, ArH, their isotopologues D_2, D_3, OD, D_2O, D_2O_2, DO_2, ArD, as well as HD, H_2D, HD_2, HDO, HDO_2, as well as their ions, apart from any other contaminants which may be present. The inclusion of these species into the plasma chemical model was decided on the basis of general chemistry in the H(D)-O-Ar system and experimental ICP-MS spectra. All supporting data can be found in the Appendix.

The equilibrium distributions of neutral and ionized plasma species are displayed in Fig. 1, a) and 1b, correspondingly. The initial stoichiometry was $H_2O/D_2O/Ar = 0.9/0.1/150$ and partial number densities were such that they satisfied the equation of state for an ideal gas at amospheric pressure. The stoichiometry reproduces the actual experimental conditions that were 20 L/min and ~130 μL/min the flow rates of Ar and water, correspondingly (also accounting for the nebulization efficiency).

The equilibrium concentrations in Fig. 1a and 1b show which polyatomic species can in principle form and which (Fig. 1, b) may be of importance for the detection of low deuterium concentrations. One infers from Fig. 1, b that likely candidates for a sensitive detection of deuterium are the species $\boldsymbol{ArD^+}, \boldsymbol{OD^+}, \boldsymbol{HD^+}$ and $\boldsymbol{D_2^+}$ (with corresponding $\boldsymbol{m/z}$ values of 42, 18, 3, and 4) that can survive high temperatures in excess of 5000 K. Please note that even though the neutral molecules $\boldsymbol{ArH}$ and $\boldsymbol{ArD}$ are very unstable and

existing only in highly excited (Ridberg) electronic states (see Appendix), their ions, $\boldsymbol{ArH^+}$ and $\boldsymbol{ArD^+}$ are stable and are formed in a significant amount. Another potential candidate for the detection of deuterium in argon ICP could be $\boldsymbol{ArD_2^+}$. However, this ion is very unstable; the force constant for this molecule (more precisely, for its hydrogen counterpart) is twice as low as that in $\boldsymbol{ArD^+}$ and the $\boldsymbol{D-D}$ ($\boldsymbol{H-H}$) bond is twice weaker than in $\boldsymbol{D_2^+}$ (H_2^+) molecule. The molecule $\boldsymbol{ArD_2^+}$ can be a degradation precursor to $\boldsymbol{ArD^+}$ [36]; for this reason it is not included in the model. One also sees by comparing Fig. 1, a) and b) that the concentration of these ions are 3-5 orders of magnitude lower than that of neutral molecules in the plasma at lower temperatures. The presence of molecular ions at high temperatures reflects the fact that protium/deuterium compounds have high bonding energies.

The validity of our computational approach was additionally confirmed by using an alternative algorithm, the open source CEA NASA software [37]. The method is based on the minimization of Gibbs free energy of the chemical system. The two algorithms predict identical mole fractions for the corresponding species. The NASA's algorithm cannot, however, be used for concentrations below 10^{-6} mole fractions; meanwhile such concentrations are still detectable by ICP-MS. On the contrary, our algorithm does not have such the limitation.

The model clearly predicted that species at mass 4 (D_2^+ and H_2D^+) and mass 42 (ArD^+) have the greatest potential for use in quantitative analytical measurements, as their predicted concentration in the plasma steadily grows with the D concentration. Both concentrations showed at least 4 orders of magnitude change as a function of D concentration, so a similar signal dynamic range can be anticipated. The concentration for ArD^+ was found to be about 10^4 times larger than the total concentration of D_2^+ and

H_2D^+, hence a significantly lower limit of detection can be predicted for analytical measurements at mass 42 than for those at mass 4.

3.2. Signal stability

One of the primary concerns related to deuterium analysis in open autosampler vials is that there would be an exchange of *D* between the sample solution and water vapor in ambient air. Also, heavy and light water have slightly different physico-chemical characteristics, thus also a different rate of evaporation. Consequently, the longer the measurement takes the more these effects could shift the deuterium concentration in the samples. Wash-in/wash-out times for sample introduction also have to be chosen carefully, as a memory effect can be expected due to the presence of residual droplets in the spray chamber. Typical, cooled Scott-type ICP-MS spray chambers have a significant dead volume, which effectively buffers pressure fluctuations in nebulizer operation and helps the formation of a finer aerosol via secondary and tertiary processes, but also provides a relatively large surface for the deposition of droplets. We also conducted experiments to assess the severity of these conditions. These experiments were only carried out with signals at masses 4 and 42, which showed the best analytical potential in the previous section.

Signal time profiles for a case when two samples with 2000 ppm and 150 ppm deuterium concentration (the latter is roughly equivalent to the natural abundance), placed in open autosampler vials, were sequentially measured (measurement time in each sample: 900 s). These profiles, shown in Fig 2., therefore represent the transition from a high to a low concentration, which can also aid the determination of necessary wash-in/wash-out times. As it can be seen, 900 s is just enough for the transition, which suggests that such very long wash-in/wash-out times are indeed required for deuterium

analysis with an ICP-MS using a standard sample introduction system. Of course, this time can be cut shorter if a lower dead volume (e.g. a cyclonic) spray chamber is used. The fact that the signal for the high concentration sample was actually lower in the second cycle than in the first cycle indicates that a detectable hydrogen isotope exchange in fact occurs between the sample and the environment during the long, 1800 s duration of the measurement cycle. According to the expectations, the signal level for the lower concentration (150 ppm) was not affected. This observation implies that best accuracy can only be achieved if the samples are kept in closed containers and are manually placed in the autosampler vial just before their measurement.

The difference between the evaporation rate for deuterated and non-deuterated water was also assessed. In this experiment, pure D_2O and H_2O were placed in standard, polypropylene autosampler vials (Agilent No. G3160-65303) and their evaporation loss was monitored using an analytical balance with a 5-second update rate for two hours at 25.5°C and 27% relative humidity. It was found that the relative evaporation loss difference during 1800 s was very small, it amounted to only about 0.05%, thus it did not effectively interfere with the deuterium concentration measurement.

Finally, signal repeatability was also tested, by cyclically measuring 2000 and 150 ppm deuterated water solutions, always placing fresh sample solutions in standard open autosampler vials just before the measurement. Signal repeatability under these conditions was 2.2% RSD at mass 42, where the signal is more sensitive, signal scatter is lower and hence the repeatability is better. This repeatability is considered acceptable for practical applications.

3.3. Spectral interference effects

Deuterium analysis via the scrutinized polyatomic species may also be subject to spectral interference. Due the extremely low mass, such interference at mass 4 is highly unlikely as it would only be possible via ^{4}He or ^{3}HeH, which can not be reasonably expected to be present. At the same time, several interferents, primarily ^{42}Ca, ^{39}KDH, may influence the analysis at mass 42. Please note that the formation of $^{40}ArH_2$ has been ruled out by the force constants (see Section 3.1. or the Appendix).

We assessed the interference from Ca and K polyatomics at mass 42 by the addition of $CaCl_2$ and KCl, respectively, in an increasing concentration to certified water samples (Fig. 3). As it can be seen, there was no significant influence of these species on the signal up to 100 µg/L – the extent of influence, if any, is within the repeatability (a couple of % RSD). Based on this it can be stated that up to at least 100 µg/L interferent concentration and for sample solutions possessing medium to high deuterium concentrations, this interference effect is negligible. At the same time, isobaric interference from ^{42}Ca, a minor isotope with an abundance of 0.647%, can occur, if a substantial concentration of calcium is present in the sample. This condition can be detected by monitoring the signal at mass 43. If calcium is present, than the less sensitive signal at mass 4 or the multiple standard addition calibration approach can be used for the analysis. It can also be added that since only <3000 mass resolution is needed to resolve the ArD signal from the ^{42}Ca signal, therefore the proposed method can probably be easily used on real samples in a high resolution ICP-MS instrument.

3.4. Optimization of plasma conditions

Analytical signals from polyatomic species may be more sensitive to plasma conditions than monoatomic ions, thus the optimization of plasma measurement conditions is important. With respect to D_2 and ArD species our plasma modeling revealed, to some

extent surprisingly, that these polyatomic ions should become more abundant in the plasma with the increase of plasma temperature (see Fig. 1). In ICP-MS, the plasma temperature in the analytical channel is known to strongly correlate with the RF forward power, but the local plasma temperature is also a function of the axial position [38], thus the choice of sampling depth also influences the local temperature at which the ions are extracted from the analytical channel. In addition, the optimal sampling position in the plasma where the concentration of polyatomic species is highest can also be different from that of monoatomic species.

In order to optimize the analytical sensitivity of signals at mass 4 and 42, we performed two-parameter experimental signal optimization involving RF forward power and plasma sampling depth, in the ranges of 1000 to 1500 W and 3 to 15 mm, respectively, using a 2000 ppm D sample. Results are very different for the two signals and are shown in Fig. 4.

At mass 42, the sampling depth has, especially at lower RF power values, a relatively small influence on the magnitude of the signal, but the signal strongly and monotonously increases with the RF power. The latter observation is in line with the projection of the plasma model in Section 3.1. The relatively small influence of the sampling depth on the signal is probably due to the fact that argon is abundant and readily available everywhere in the plasma for the formation of ArD^+. The optimal conditions were 1500 W power and 10 mm sampling depth.

The signal at mass 4 behaves differently. The concentration of D_2 strongly increases with the decrease of plasma sampling depth. This can probably be explained by the enhanced diffusion rate of this very light ion, according to Graham's law, out of the analytical channel [38, 39], which dictates the use of a sampling depth as small as possible. The local plasma temperature is also higher close to the induction coil, unless

too close to the initial radiation zone, in the analytical channel [38]. At the same time, the signal is highest for medium RF powers, which suggests that D_2 is thermodynamically less stable than *ArD*. The optimal conditions were 1200 W power and 3 mm sampling depth.

3.5. Analytical performance

Calibration plots recorded at conditions optimal for deuterium analysis can be seen in Fig. 5. The plots display excellent linearity for concentrations upwards from ppm levels, the dynamic range is 4-5 orders of magnitude for mass 4 and 42, respectively. For both masses, a positive deviation from linearity can be observed at the low end, which is probably due to the contribution from DH_2 and ArH_2 species, dominant at low D concentrations. The limit of detection (LOD) calculated by the three sigma approach was found to be 78 ppm at mass 4, and 3 ppm at mass 42. In the delta notation used in geological, biological and environmental analysis, these LOD values are equivalent to δD -496.02‰ and -980.74‰, respectively on the VSMOW (Vienna Standard Mean Ocean Water) scale [40]. These LOD values allow the measurement of deuterium concentrations at around or above the natural level, up to nearly 100% or 1 Mio ppm (6.5 Mio ‰). This analytical range, especially for the signal at mass 42 is much wider than typically measured δD values for natural compounds, ranging from ca. -200 to +50 [40]. With a signal repeatability about 2.2% RSD, the measurement under the presently investigated conditions can not be more accurate than about 15‰, which significantly poorer than the state-of-the-art IRMS or IRIS accuracy data of <1‰ [8, 9]. However, the accuracy of this ICP-MS method can be significantly improved with the use of a fast-rinse sample introduction system and septum-closed vials. The analytical time is already short (ca. 15 minutes) as it does not require conversion or reduction of the

sample to gas, and this time can also be further decreased by employing the mentioned improvements in sample introduction.

4. Conclusions

Our approach of using the signal from deuterium-containing polyatomic species (D_2 and ArD) for analytical purposes is new and unique - it has not been formerly suggested, according to our best knowledge, in the ICP-MS literature. By incorporating available kinetic and thermodynamic data, we have created a plasma chemistry model for the assessment of the analytical potential or influence of relevant (hydrogen, oxygen and argon-containing) polyatomic species and validated our findings by experiments. This approach allows the application of the method on any ICP-MS instruments, even on those where the mass analyzer does not work for masses as low as 2. The only spectral interference that may influence the results obtained on mass 42 is from calcium, but even this was found not to interfere for up to 100 ppb calcium concentrations in samples with 2000 ppm D. On high resolution ICP-MS instruments, this interference can be easily resolved.

Our analytical method for deuterium determination is also quick and sensitive for practical deuterium measurements, and only requires a few mL of liquid samples. Due to the action of ICP plasma and mass spectrometry detection, principally the measurement can be selectively performed on almost any sample that can be introduced into an ICP-MS, without the need for reducing/converting the sample. The dynamic range is 4-5 orders of magnitude, extending from the ppm-level to near full deuteration, thereby easily covering δD values in any natural waters or deuterium-enriched samples. In case of samples that require sample preparation or dilution, chemicals with certified deuterium content need to be used – such chemicals, including

solvents, acids, heavy water, etc. are commercially available from specialized companies worldwide. ICP-MS can also be combined with flowing sample preparation systems, similar to IRMS or IRIS for isotope analysis. Solid samples (e.g. food or other organics) may also be directly analyzed by our method using laser ablation sample introduction. This latter possibility is currently being investigated in our laboratory.

The analytical capabilities of our method represent a combination of favorable characteristics. The speed of analysis and level of accuracy is comparable to refractive index or FTIR measurements. The ability of using various sample types and the much better selectivity of ICP-MS also makes this method superior over other methods. At the same time, the limit of detection and dynamic range are more comparable to those of the tedious, but very accurate IRMS or IRIS approaches. The accuracy of our method, when executed on a quadrupole mass analyzer, single collector ICP-MS, like in our experiments, is of course not in par with IRMS, IRIS or SNIF-NMR methods, but it is believed to be improvable by using more sophisticated sample introduction systems (e.g. in-torch microconcentric nebulizer and an autosampler working with septum-sealed vials) or on sector-field MC-ICP-MS instruments (e.g. by monitoring ArH and ArD signal ratios). Hence we think that ICP-MS can become a valuable and practical addition to the list of methods applicable to hydrogen stable isotope analysis in several application fields.

Acknowledgements

The authors thank the valuable assistance provided by Sára Bálint and Ádám Bélteki (both of the University of Szeged, Hungary) in the execution of some of the experiments described. The authors also acknowledge the financial support from the National Research, Development and Innovation Office (through project EFOP-3.6.2-16-2017-

00005 „Ultrafast physical processes in atoms, molecules, nanostructures and biology structures“) of Hungary. Igor Gornushkin thanks Prof. U. Panne and Dr. K. Rurack for their everlasting support.

References

[1] M.F. Estep, T.C. Hoering: Biogeochemistry of the stable hydrogen isotopes, Geochimica et Cosmochimica Acta, Volume 44, Issue 8, 1980, Pages 1197-1206.

[2] S. Benson, C. Lennard, P. Maynard, C. Roux: Forensic applications of isotope ratio mass spectrometry — a review, Forensic Science International, Volume 157, Issue 1, 2006, Pages 1-22.

[3] S. Kelly, K. Heatonband, J. Hoogewerff: Tracing the geographical origin of food: The application of multi-element and multi-isotope analysis, Trends in Food Science & Technology, Volume 16, Issue 12, 2005, Pages 555–567.

[4] C.K. Gupta: Materials in nuclear energy applications: Volume I, Chapter 2, Nuclear fission reactor, 1st Edition, 2018, CRC Press, Boca Raton, FL, USA

[5] H. Günther: NMR Spectroscopy: Basic Principles, Concepts and Applications in Chemistry, 3rd Edition, 2013, Wiley-VCH, Weinheim, Germany

[6] G. Somlyai, G. Laskay, T. Berkényi, Z. Galbács, G. Galbács, S.A. Kiss, Gy. Jákli, G. Jancsó: The biological effects of deuterium-depleted water, a possible new tool in cancer therapy, Journal of Oncology, Volume 30, Issue 4, 1998, Pages 91-94.

[7] R.A. Werner, W.A. Brand: Referencing strategies and techniques in stable isotope ratio analysis – a review, Rapid Communications in Mass Spectrometry, Volume 15, Issue 7, 2001, Pages 501-519.

[8] R. van Geldern, J.A.C. Barth: Optimization of instrument setup and post-run corrections for oxygen and hydrogen stable isotope measurements of water by isotope ratio infrared spectroscopy (IRIS), Limnology and Oceanography: Methods, Volume 10, Issue 12, 2012, Pages 1024–1036.

[9] A.G. West, G.R. Goldsmith, P.D. Brooks, T.E. Dawson: Discrepancies between isotope ratio infrared spectroscopy and isotope ratio mass spectrometry for the stable isotope analysis of plant and soil waters, Rapid Communications in Mass Spectrometry, Volume 24, Issue 14, 2010, Pages 1948–1954.

[10] G.J. Martin, S. Akoka, M.L. Martin: SNIF-NMR: Part 1: Principles, in: G.A. Webb (Ed.), Modern Magnetic Resonance, 2nd Edition, 2008, Springer, Berlin, Germany

[11] S.P. Best, A.J. Bloodworth, R.J.H. Clark, H.J. Eggelte: Detection of hydrogen, hydrogen-deuterium molecule (HD), and deuterium by Raman spectroscopy: a powerful aid for the elucidation of reaction mechanisms, Journal of the American Chemical Society, Volume 107, Issue 9, 1985, Pages 2626-2628.

[12] C. Genty, R. Schott: Quantitative Analysis for the Isotopes of Hydrogen- H_2, HD, HT, D_2, DT, and T_2 - by gas chromatography, Analytical Chemistry, Volume 42, Issue 1, 1970, Pages 7-11.

[13] A. Rein, F. Higgins: Application of the Agilent 4500 Series FTIR to the Stable Isotope Technique for Assessing Intake of Human Milk in Breastfed Infants, 2014, Agilent Technologies, Application note 5991-3531EN.

[14] A. D'Ulivo, M. Onor, E. Pitzalis, R. Spiniello, L. Lampugnani, G. Cristoforetti, S. Legnaioli, V. Palleschi, A. Salvetti, E. Tognoni: Determination of the deuterium/hydrogen ratio in gas reaction products by laser-induced breakdown spectroscopy, Spectrochimica Acta Part B: Atomic Spectroscopy, Volume 61, Issue 7, 2006, Pages 797–802.

[15] A.A. Bol'shakov, X. Mao, J.J. González, R.E. Russo: Laser ablation molecular isotopic spectrometry (LAMIS): current state of the art, Journal of Analytical Atomic Spectrometry, Volume 31, Issue 1, 2016, Pages 119-134.

[16] F. Vanhaecke, P. Degryse: Isotopic analysis: fundamentals and applications using ICP-MS, 1st Edition, 2012, Wiley-VCH, Weinheim, Germany

[17] E. Albalat, P. Telouk, V. Balter, T. Fuji, V.P. Bondanese, M-L. Plissonnier, V. Vlaeminck-Guillem, J. Baccheta, N. Thiam, P. Miossec, F. Zoulim, A. Puisieuxgand, F. Albaréde: Sulfur

isotope analysis by MC-ICP-MS and application to small medical samples, Journal of Analytical Atomic Spectrometry, Volume 31, Issue 4, 2016, Pages 1002-1011.

[18] S.H. Tan, G. Horlick: Background Spectral Features in Inductively Coupled Plasma/Mass Spectrometry, Applied Spectroscopy, Volume 40, Issue 4, 1986, Pages 445-460.

[19] R.S. Houk, V.A. Fassel, G.D. Flesch, H.J. Svec, A.L. Gray, C.E. Taylor, Inductively coupled argon plasma as an ion source for mass spectrometric determination of trace elements, Analytical Chemistry, Volume 52, Issue 14, 1980, Pages 2283–2289.

[20] N.M. Reed, R.O. Cairns, R.C. Hutton, Y. Takaku, Characterization of polyatomic ion interferences in inductively coupled plasma-mass spectrometry using a high resolution mass spectrometer, Journal of Analytical Atomic Spectrometry, Volume 9, Issue 8, 1994, Pages 881–896.

[21] T.W. May, R.H. Wiedmeyer: A table of polyatomic interferences in ICP-MS, Atomic Spectroscopy, Volume 19, Issue 5, 1998, Pages 150-155.

[22] R.S. Houk, N. Praphairaksit, Dissociation of polyatomic ions in the inductively coupled plasma, Spectrochimica Acta Part B: Atomic Spectroscopy, Volume 56, Issue 7, 2001, Pages 1069–1096.

[23] J.W. Ferguson, R.S. Houk: High resolution studies of the origins of polyatomic ions in inductively coupled plasma-mass spectrometry, Part I. Identification methods and effects of neutral gas density assumptions, extraction voltage, and cone material, Spectrochimica Acta Part B: Atomic Spectroscopy, Volume 61, Issue 8, 2006, Pages 905–915.

[24] N.S. Nonose, N. Matsuda, N. Fudagawa, M. Kubota, Some characteristics of polyatomic ion spectra in inductively coupled plasma-mass spectrometry, Spectrochimica Acta Part B: Atomic Spectroscopy, Volume 49, Issue 10, 1994, Pages 955–974.

[25] N. Nonose, Formation of interfering polyatomic ion species in ICP-MS, Journal of the Mass Spectrometry Society of Japan, Volume 45, Issue 1, 1997, Pages 77–89.

[26] A.A. van Heuzen, N.M.M. Nibbering, Elemental composition and origin of (polyatomic) ions in inductively coupled plasma mass spectrometry disclosed by means of isotope exchange

experiments, Spectrochimica Acta Part B: Atomic Spectroscopy, Volume 48, Issue 8, 1993, Pages 1013–1021.

[27] S.D. Tanner, V.I. Baranov, D.R. Bandura: Reaction cells and collision cells for ICP-MS: a tutorial review, Spectrochimica Acta Part B: Atomic Spectroscopy, Volume 57, Issue 9, 2002, Pages 1361-1452.

[28] L. Balcaen, E. Bolea-Fernandez, M. Resano, F. Vanhaecke: Inductively coupled plasma – Tandem mass spectrometry (ICP-MS/MS): A powerful and universal tool for the interference-free determination of (ultra)trace elements – A tutorial review, Analytica Chimica Acta, Volume 894, Issue 24, 2015, Pages 7-19.

[29] F.G. Smith, R.S. Houk, Alleviation of polyatomic ion interferences for determination of chlorine isotope ratios by inductively coupled plasma mass spectrometry, Journal of the American Society for Mass Spectrometry, Volume 1, Issue 4, 1990, Pages 284–287.

[30] M.V. Zoriy, L. Halicz, M.E. Ketterer, C. Pickhardt, P. Ostapczuk, J.S. Becker, Reduction of UH^+ formation for $^{236}U/^{238}U$ isotope ratio measurements at ultratrace levels in double focusing sector field ICP-MS using D_2O as solvent, Journal of Analytical Atomic Spectrometry, Volume 19, Issue 3, 2004, Pages 362–367.

[31] S.V. Shabanov, I.B. Gornushkin: Modeling chemical reactions in laser-induced plasmas, Applied Physics A, Volume 121, Issue 3, 2015, Pages 1087-1107.

[32] S.V. Shabanov, I.B. Gornushkin: Anions in laser-induced plasmas, Applied Physics A, Volume 122, Issue 7, 2016, Article ID 676.

[33] S.V. Shabanov, I.B. Gornushkin: Chemistry in laser-induced plasmas at local thermodynamic equilibrium, Applied Physics A, Volume 124, Issue 10, 2018, Article ID 716

[34] J.M. Mermet: Fundamental principles of inductively coupled plasma, Chapter 2, in: S.J. Hill (Ed.), Inductively coupled plasma spectrometry and its applications, 2nd Edition, 2007, Blackwell Publishing Ltd., Hoboken, NJ, USA, Pages 27-60.

[35] K.J.R. Rosman, P.D.P. Taylor: Isotopic compositions of elements 1997 (Technical Report), Pure and Applied Chemistry, Volume 70, Issue 1, 1998, Pages 217-235.

[36] R.A. Theis, W.J. Morgan, R.C. Fortenberry: ArH_2^+ and NeH_2^+ as global minima in the $Ar^+/Ne^+ + H_2$ reactions: energetic, spectroscopic, and structural data, Monthly Notices of the Royal Astronomical Society, Volume 446, Issue 1, 2015, Pages 195–204.

[37] https://cearun.grc.nasa.gov

[38] A. Bogaerts, M. Aghaei: Inductively coupled plasma-mass spectrometry: insights through computer modeling, Journal of Analytical Atomic Spectrometry, Volume 32, Issue 2, 2017, Pages 233–261.

[39] K. Niemax: Considerations about the detection efficiency in inductively coupled plasma mass spectrometry, Spectrochimica Acta Part B: Atomic Spectroscopy, Volume 76, Honoring Issue: A Collection of Papers on Plasma and Laser Spectrochemistry. Dedicated to Gary M. Hieftje on the occasion of his 70th birthday, 2012, Pages 65-69.

[40] W.G. Mook: Environmental isotopes in the hydrological cycle: Principles and applications, Volume 1., 2001, International Atomic Energy Agency, UNESCO

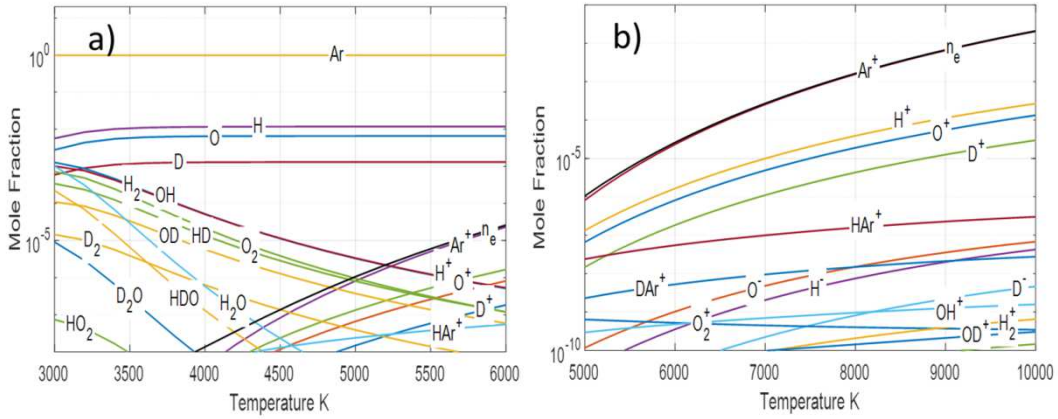

Figure 1. Equilibrium composition of the $\boldsymbol{H_2O/D_2O/Ar}$ plasma as a function of temperature; a) mole ratio $\boldsymbol{H_2O/D_2O/Ar = 0.9/0.1/150}$, neutrals; b) same, ions; Calculations were made for atmospheric pressure.

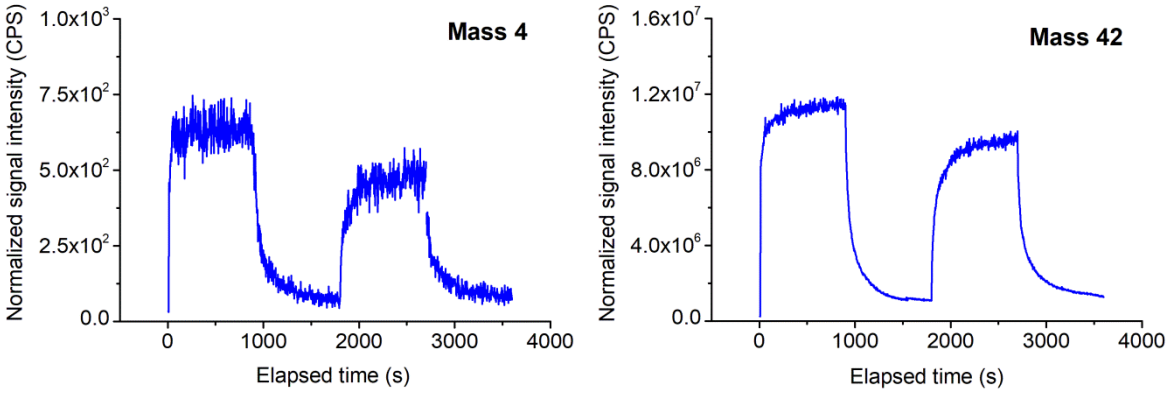

Figure 2. Signal time profiles for an alternating measurement of water samples with 2000 and 150 ppm deuterium concentration. Signals were normalized to that of ^{6}Li and ^{45}Sc, respectively, in order to correct for any instrumental drift.

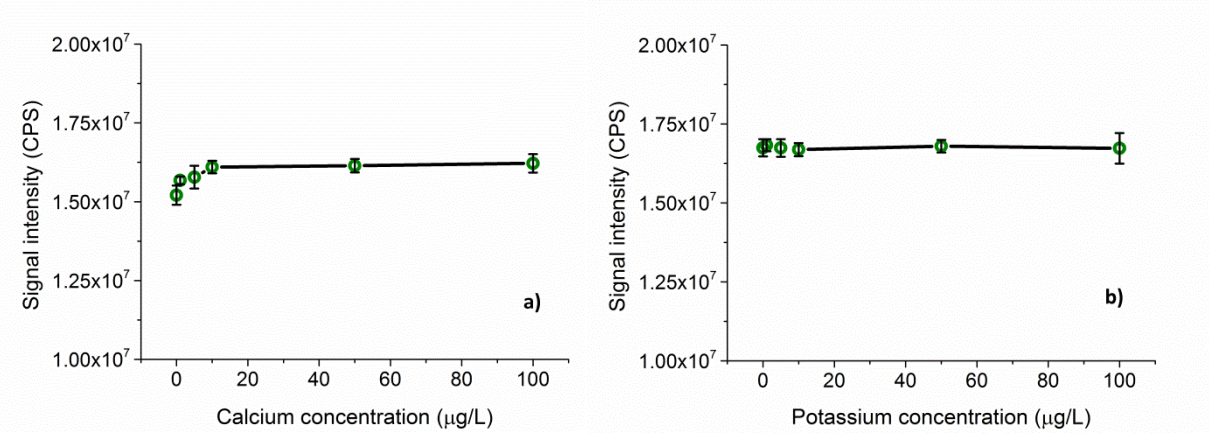

Figure 3. Assessment of potential spectral interference on the signal at mass 42 from Ca (left) and K (right) polyatomic species in a 2000 ppm D water sample. Please note that Ca and K concentrations are expressed here on a mass per volume basis. Error bars indicate standard deviations based on five replicate measurements.

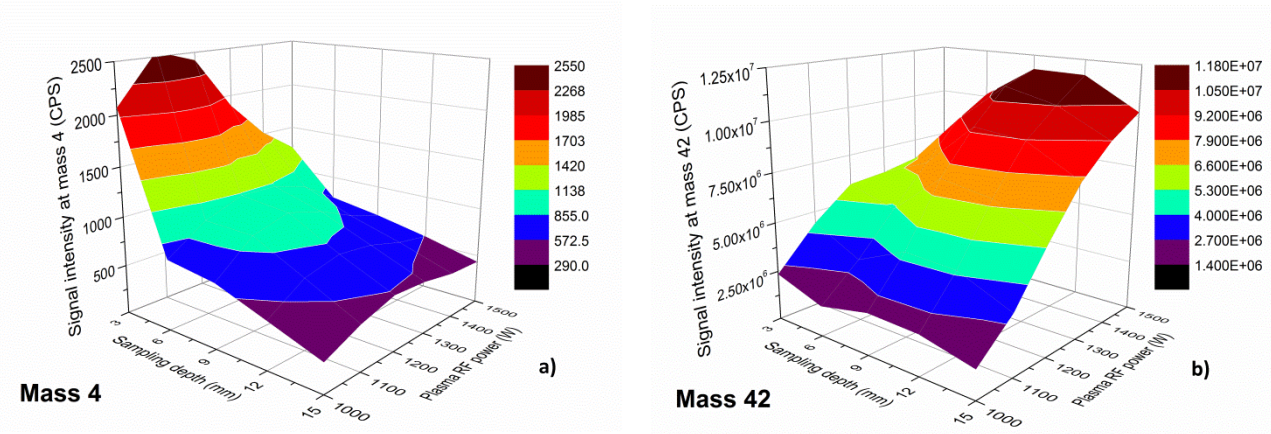

Figure 4. Optimization of plasma conditions for maximizing the signals at mass 4 and 42.

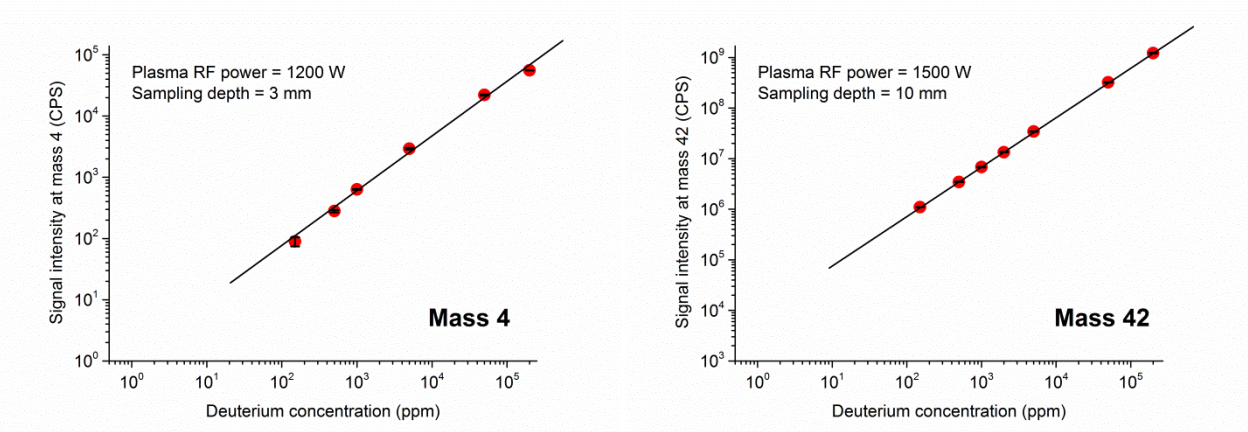

Figure 5. Calibration plots under optimal conditions for deuterium analysis at masses 4 and 42. Error bars indicate standard deviations based on five replicate measurements.

Appendix

Partition functions for molecules and their ions

The partition functions for *diatomic* molecules and their ions used in simulations are calculated using the equation of Tatum [1]

$$U(T) = exp\left[\frac{hc}{kT}\left(\frac{1}{2}\omega_{e_1} - \frac{1}{4}\omega_{e_1 x_{e_1}}\right)\right]\sum_e \sum_{v=0}^{N_e} \frac{g_e kT}{\sigma hc}\left[B_e - \alpha_e\left(v+\frac{1}{2}\right)\right]^{-1} \times exp\left\{-\frac{hc}{kT}\left[\omega_e\left(v+\frac{1}{2}\right) - \omega_e x_e\left(v+\frac{1}{2}\right)^2 + T_e\right]\right\} \quad \text{(A1)}$$

Here T_e is the electronic state energy ($T_0 = 0$ for the ground state), ω_e is the vibration frequency, $\omega_e x_e$ is the anharmonicity, B_e is the rotational constant, α_e is the rotation-vibration coupling, and σ is the symmetry number that accounts for the number of indistinguishable orientations of a molecule. The overall factor in the sum (A1) is the vibrational zero-point-energy (ZPE) that is the energy difference between the vibrational ground state and the lowest point on the potential energy surface. The maximal vibrational number N_e for each electronic state is limited by the depth of the potential well is given by $N_e = \frac{1}{2}(\frac{\omega_e}{\omega_e x_e} - 1)$.

The partition functions for *tri-* and *four-atomic* molecules and their ions are calculated using the Born-Oppenheimer approximation. The approximation assumes that the modes of molecular motion (vibrational, rotational, translational) are independent (decoupled) from each other and thus the total partition function can be factorized into a product of individual partition functions. This approach does not account for anharmonicity and, hence, permits a representation of the sums over vibrational energies in a closed form using the geometric series. For polyatomic molecules the partition function is calculated via [2, 3]

$$U(T) = \frac{1}{\sigma}\sum_e U_e^{rot}(T) g_e exp\left(\frac{T_e}{T}\right) \prod_{j=1}^{M_e} \frac{1}{1-exp\left(-\frac{hc\omega_{e_j}}{kT}\right)} \quad \text{(A2)}$$

where $U_e^{rot}(T)$ is the rotational partition function which is $U_e^{rot}(T) = \left(\frac{kT}{hc}\right)^{\frac{3}{2}}\left(\frac{\pi}{ABC}\right)^{\frac{1}{2}}$ for non-linear polyatomic molecules with three rotational constants A, B, and C and the value $U_e^{rot}(T) = \frac{kT}{chB_e}$ for linear polyatomic molecules with one rotational constant B_e. Each rotational constant is proportional to the moment of inertia of the molecule about the corresponding principal axis of the moment of inertia tensor, e.g. $A = \frac{h}{8\pi^2 c I_A}$. Therefore, the rotational constants can easily be calculated if the moments of inertia are known or calculated from molecular geometry and spectroscopic constants. The number of vibrational frequencies is $M_e = 3N - 6$ for non-linear polyatomics and $M_e = 3N - 5$ for linear polyatomics with N being the number of constituent atoms. Note the rotational partition function $U_e^{rot}(T)$ depends on an electronic state e because some molecules change their geometry (e.g. from bent to linear) depending on the electronic excitation. An example is the BCl_2 molecule which is bent in its ground electronic state and stretched (linear) in the excited electronic state.

H, H^+, H^-, D, D^+, D^-

The partition function for H is taken from [4]. The ion H^+ has no electrons; its "electronic" partition function is therefore 1. The ground state of the anion H^- has two electrons with two oppositely oriented spins; its degeneracy is 1. The anion has no excited states with energies below the ionization (electron affinity) energy $I(H^-) = 0.75\ eV$ and therefore the full electronic partition function of H^- is also 1. The data for electronic partition functions of deuterium repeat that for hydrogen.

O, O^+, O^-

Partition functions for O and O^+ are taken from [1]. The ground state of O^- has configuration $1s^2 2s^2 2p^5$ which allows terms $^2\mathrm{P}_{3/2}$ and $^2\mathrm{P}_{1/2}$ with degeneracies 4 and 2, correspondingly. Existence of excited states of O^- is unlikely [5]; the partition function for O^- is therefore 6.

$H_2, H_2^+, H_2^-, D_2, D_2^+, D_2^-, HD, HD^+, HD^-$

The partition function for H_2 is conveniently calculated using the recent polynomial approximation [6]. For H_2^+, the electronic states $X^2\Sigma_g^+$, $B^2\Sigma_g^+$, and $C^2\Pi_u$ given in [7] were used to calculate the partition function via the spectroscopic constants using Eq. (A1). The ground state of the anion H_2^- is metastable; that is, there exists no bound anion state [8]. Only the ground states $X^1\Sigma_g^+$ and $X^2\Sigma_g^+$ for D_2 and HD and D_2^+ and HD^+, correspondingly are accounted for because the higher states have energies $\sim 11\ eV$ that greatly exceeds the dissociation energies of these molecules. The data are from [8].

$H_3, H_3^+, H_3^-, D_3, D_3^+, D_3^-, H_2D, H_2D^+, H_2D^-, D_2H, D_2H^+, D_2H^-$

The molecule H_3 and isotopologues D_3, H_2D and D_2H are the most stable in an equilateral triangular shape; they belong to the D_{3h} symmetry group with the symmetry number $\sigma = 6$. They have repulsive ground states and can only exist in excited states. The dissociation energies for these molecules are set to zero while the data for the ionization energy, $IP(H_3) = 3.67\ eV$ and several excited electronic states are taken from [9]. In contrary, the molecules H_3^+, D_3^+, H_2D^+ and D_2H^+ are stable in the ground state and also have the stable triangular configuration. For H_3^+, there exist one totally symmetrical $^1A'$ and doubly degenerate vibrations E_1' [10]. The data for the vibration frequencies 3179.9 and 2521.3 cm^{-1} are from [9]. The corresponding frequencies for

D_3^+, $\omega_1 = 2300.84\ cm^{-1}$ ($^1A'$ ring breathing) and $\omega_2 = 1834.67\ cm^{-1}$ (E_1' deformation) are from [11]. The rotational constants for D_3^+ are assumed to be the same as for H_3^+ [9]. The data for the ground state $\tilde{X}^1A_1'$ of H_3^+ are from [9] and for the ground states of H_2D^+ and D_2H^+ are from [12]. The rotational constants for D_2H^+ (available in [12]) are repeated for H_2D^+ considering the similarity of these molecules. The anions H_3 and corresponding isotopologues are the weakly bound molecules [13]; it is difficult to detect them experimentally [14]. They are created as transient structures in collisional processes and have relevance to processes in cold interstellar clouds. Even though ab initio data for these molecules exist [13, 15], they are neglected for the present study.

O_2, O_2^+, O_2^-

The partition functions for all three species are from Herzberg [7]. For O_2^-, the only stable state is $X^2\Pi_g$ [16].

$OH, OH^+, OH^-, OD, OD^+, OD^-$

The partition function for OH and dissociation energy $D(OH) = 4.39\ eV$ are from [7]. The ionization energy $I(OH) = 13.02\ eV$ is from NIST and the electron affinity $EA(OH) = 1.83\ eV$ is from [17]. Five electronic states $X^3\Sigma^-$, $a^1\Delta$, $A^3\Pi$, $b^1\Sigma^+$, and $A^1\Pi$ [18] are used to calculate the partition function of OH^+ and three electronic states $X^3\Sigma^-$ [19] and $a^1\Delta$, $A^3\Pi$ [20] to calculate the partition function of OH^-. The data for OD, OD^+, OD^- are from [7].

$H_2O, H_2O^+, H_2O^-, D_2O, D_2O^+, D_2O^-, HDO, HDO^+, HDO^-$

The water molecule has C_{2v} symmetry. Its ionization and dissociation energies are $I(H_2O) = 12.62\,eV$ and $D(H_2O) = 9.5\,eV$ [9], correspondingly. Only the ground state X^1A_1 is considered because the first excited state A^1B_1 lies at 6.67 eV that exceeds the bond strength $D(H-OH) = 5.11\,eV$ [9]. The H_2O^+ cation has three electronic states X^2B_1, A^2A_1, and B^2B_2 each of which has different geometry. The ground state X^2B_1 has the angle $\angle(H-O-H) = 110.46^o$ and the bond lengths $r_{O\_H} = 1.19$ Å, the state A^2A_1 is linear with the bond length $r_{O\_H} = 0.98$ Å, and the state B^2B_2 is strongly bent with $\angle(H-O-H) = 54.98^o$ and $r_{O\_H} = 1.14$ Å [21]. The vibration frequencies ω_1, ω_2, and ω_3 for these states are from [9] and the rotational constants A, B, and C are calculated from the molecular geometry. A single H_2O molecule cannot bind an electron, thus $EA(H_2O) = 0$; it can form stable anions only in clusters [8].

The ionization energy $I(D_2O) = 12.64\,eV$ is from [22], the dissociation energy $O-D$ of 4.453 eV is from [23], and $DO-D$ bond strength was assumed to be the same as in a H_2O molecule thus given the total dissociation energy $D(D_2O) = 9.57\,eV$. The ground state frequencies 2671, 1178, and 2788 cm^{-1} and the rotational constants 15.42, 7.27, and 4.85 cm^{-1} are found in [11]. The values T_e for the three lowest electronic states of D_2O +, 0, 10456, and 37430 cm^{-1} are also from NIST [11], the vibration frequencies and rotational constants are from [22] and [24], correspondingly. Electron affinity of D_2O is also zero.

The ionization energy $IP(HDO) = 12.63\,eV$ and symmetry is C_{2v} [11]. The vibration frequencies and rotational constants are from [11]. The data for HDO^+ are assumed to be identical with H_2O^+. Electron affinity $EA(HDO) = 0$.

$HO_2, HO_2^+, HO_2^-, DO_2, DO_2^+, DO_2^-$

The radical HO_2 is important in combustion and atmospheric chemistry. It belongs to the C_S symmetry group ($\sigma = 1$). Its dissociation and ionization energies are $D(HO_2) = 7.2\ eV$ and $I(HO_2) = 11.35\ eV$, respectively [25]. The electron affinity is 1.08 eV [17]. The ground state is $\tilde{X}^2A''$ with the angle between $H-O$ and $O-O$ bonds $\angle(H-O-O) = 104.5^o$ and the bond lengths $r_{H\_O} = 0.98$ Å and $r_{O\_O} = 1.33$ Å [25]. The vibration frequencies are 3436, 1392, and 1098 cm^{-1}[26], the rotational constants are 20.36, 1.12, and 1.06 cm^{-1} [27]. The molecule has an excited state $\tilde{A}^2A'$ with $T_e = 7030\ cm^{-1}$ with frequencies 3959, 1254, and 968 cm^{-1} [28] and rotational constants 20.49, 1.02, and 0.97 cm^{-1} [27]. There exist higher electronic states $(2)^2A''$ and $(2)^2A'$ but they are unimportant because their excitation energies 5.9 eV and 6.5 eV [28] are higher than the dissociation energy $D(HO_2)$. The cation HO_2^+ has three lowest electronic states $\tilde{X}^3A''$, $\tilde{A}^1A'$, and $\tilde{A}^1A''$. The T_e values calculated relative to the $\tilde{X}^3A''$ ground state are 1185 cm^{-1} (1670 cm^{-1} [29]) and 9034 cm^{-1} [30]. The vibrational frequencies 3030, 1414, 1063 cm^{-1} and 2986, 1462, 1395 cm^{-1} and rotation constants 21.90, 1.28, 1.21 cm^{-1} and 20.45, 1.33, 1.25 cm^{-1} for the first two states are from [30]; the vibrational frequencies 3131, 1090, 1330 cm^{-1} and rotation constants 21.22, 1.26, 1.19 cm^{-1} for the third state are from [29]. The anion HO_2^- has ground state $\tilde{X}^1A'$ with vibrational frequencies 3827, 1099, and 745 cm^{-1} [31]. The rotational constants 19.31, 0.86, and 0.82 cm^{-1} are calculated from the geometrical data $\angle(H-O-O) = 97.34^o$, $r_{H\_O} = 0.96$ Å, and $r_{O\_O} = 1.53$ Å [31].

The ionization potential and dissociation energy for DO_2 are assumed to be the same as for HO_2. The electron affinity $EA = 1.077\ eV$ is from [17]. The vibration frequencies 2531.1, 1024.6, and 1121.5 $cm^{-1}$for the ground state $\tilde{X}^2A''$ are from NIST, the rotational constants 11.166, 1.056, and 0.962 cm^{-1} are from [32]. The data for DO_2^+ and DO_2^- repeat that for HO_2^+ and HO_2^-.

$H_2O_2, H_2O_2^+, H_2O_2^-, D_2O_2, D_2O_2^+, D_2O_2^-, HDO_2, HDO_2^+, HDO_2^-$

Neutral H_2O_2 has a "open book" C_2 structure with the ground state $\tilde{X}^1A$, vibrational frequencies $3653, 1460, 1028, 356, 3655, 1333\ cm^{-1}$ and rotational constants 9.8, 0.87, and $0.83\ cm^{-1}$[25]. The unusual reactivity of hydrogen peroxide is attributed to the weakness of the $O-O$ bond, $D(HO-OH) = 2.1\ eV$ [33]. The overall dissociation energy of H_2O_2 is therefore $D(HOOH) = D(HO-OH) + 2D(O-H) = 2.1eV + 2 \times 4.39\ eV = 10.88\ eV$. The ionization energy is $I(H_2O_2) = 10.63\ eV$ [25]. The ground state of $H_2O_2^+$ is $\tilde{X}^2B_g$, it is trans-planar and has full C_{2h} symmetry. The vibrational frequencies are $3337, 1557, 1395, 867, 3295, 1282\ cm^{-1}$ and rotational constants are 9.7, 1.0, and $0.93\ cm^{-1}$[25]. H_2O_2 has no positive electron affinity; electron attachment requires 2.5 eV energy [34]. The data for $D_2O_2, D_2O_2^+, D_2O_2^-$ reproduce that for $H_2O_2, H_2O_2^+, H_2O_2^-$. Both hydrogen and deuterium peroxides are expected to be present in the plasma at very low concentrations; the detailed chemical differences are therefore unimportant. The same assumption is made with respect to the mixed molecules HDO_2, HDO_2^+, HDO_2^-.

$ArH, ArH^+, ArH^-, ArD, ArD^+, ArD^-$

ArH is an extremely weakly bound molecule, $D(ArH) = 0.0042\ eV$ [35]; it supports no bound vibrational levels. However, the bound excited states of this molecule do exist and three of them, $2^2\Sigma^+, 1^2\Pi$, and $3^2\Sigma^+$ are taken into account. The T_e values for these states, 52430, 55168, and 55330 cm^{-1}, correspondingly are estimated from the graphs in [36], the spectroscopic constants $\omega_e, \omega_e x_e, B_e$, and α_e are from [37] and [7]. The excited states of ArH from Rydberg series approach the ground state of ArH^+ [37], therefore, the energy of the ground state of ArH^+ is taken as the ionization energy of

ArH. This energy was also estimated from the graphs in [36] and gave the value 9.56 eV. In contrast to ArH, ArH^+ is a strongly bound molecule with the dissociation energy as high as $D(ArH^+) = 4.02\,eV$ [38]. The vibration frequency $2775.19\,cm^{-1}$ and $B_e = 10.52\,cm^{-1}$ are from [7]; the remaining spectroscopic constants are calculated.

The data for the excited states $A^2\Sigma^+, B^2\Pi$ of ArD are from [7] and for the ground state $X^1\Sigma^+$ of ArD^+ from [39]. The negative ions ArH^- and ArD^- are neglected.

References for the Appendix:

[1] J.B. Tatum: Accurate Partition Functions and Dissociation Equilibrium Constants of Diatomic Molecules of Astrophysical Interest, Publications of the Dominion Astrophysical Observatory, Volume 13, Issue 1, 1966, Pages 1-17.

[2] P.W. Atkins, J. de Paula: Physical Chemistry, Focus 17: Chemical Kinetics, 11th Edition, 2018, Oxford University Press, Oxford, United Kingdom

[3] A.W. Irwin: The partition functions of JANAF polyatomic molecules that significantly affect the stellar atmospheric equation of state, Astronomy and Astrophysics Supplement Series, Volume 74, Issue 1, 1988, Pages 145-160.

[4] H.-W. Drawin, P. Felenbok: Data for Plasma in Local Thermodynamic Equilibrium, 1965, Gaunthier-Villars, Paris, France

[5] B. Kivel: Excited States of Negative Ions of Atomic Oxygen, Physical Review, Volume 152, Issue 1, 1966, Pates 21-25.

[6] A. Popovas, U.G. Jørgensen: Partition functions - I. Improved partition functions and thermodynamic quantities for normal, equilibrium, and ortho and para molecular hydrogen, Astronomy & Astrphysics, Volume 595, 2016, Article number A130

[7] K.P. Huber, G. Herzberg: Molecular Spectra and Molecular Structure, 1979, Van Nostrand Reinhold Co., New York, USA

[8] J. Simons, K.D. Jordan: Ab initio electronic structure of anions, Chemical Reviews, Volume 87, Issue 3, 1987, Pages 535-555.

[9] G. Herzberg: Molecular spectra and molecular structure III (Electronic spectra and electronic structure of polyatomic molecules), 1966, Krieger Publishing Co., Malabar, FL, USA

[10] H. Figger, W. Ketterle, H. Walther: Spectroscopy of triatomic hydrogen, Zeitschrift für Physik D Atoms, Molecules and Clusters, Volume 13, Issue 2, 1989, Pages 129-137.

[11] https://cccbdb.nist.gov/exp2x.asp

[12] J. Tennyson, B.T. Sutcliffe: A calculation of the rovibrational spectra of the H_3^+, H_2D^+ and D_2H^+ molecules, Molecular Physics, Volume 56, Issue 5, 1985, Pages 1175 -1183.

[13] M. Ayouz, O. Dulieu, R. Guérout, J. Robert, V. Kokoouline, Potential energy and dipole moment surfaces of H_3^- molecule, The Journal of Chemical Physics, Volume 132, 2010, Article ID 194309

[14] J. Stärck W. Meyer: Ab initio potential energy surface for the collisional system H^- + H_2 and properties of its van der Waals complex, Chemical Physics, Volume 176, Issue 1, 1993, Pages 83-95.

[15] M. Ayouz, O. Dulieu, J. Robert: Resonant States of the H_3^- Molecule and Its Isotopologues D_2H^- and H_2D^-, The Journal of Physical Chemistry A, Volume 117, Issue 39, 2013, 9941–9949.

[16] K. M. Ervin, I. Anusiewicz, P. Skurski, J. Simons, W.C. Lineberger: The Only Stable State of O_2^- Is the X $^2\Pi_g$ Ground State and It (Still!) Has an Adiabatic Electron

Detachment Energy of 0.45 eV. The Journal of Physical Chemistry A, Volume 107, Issue 41, 2003, Pages 8521-8529.

[17] J.C. Rienstra-Kiracofe, G.S. Tschumper, H.F. Schaefer, S. Nandi, G.B. Ellison: Atomic and Molecular Electron Affinities: Photoelectron Experiments and Theoretical Computations, Chemical Reviews, Volume 102, Issue 1, 2002, Pages 231-282.

[18] D.M. Hirst, M.F. Guest: An ab initio study of the excited states of OH^+, Molecular Physics, Volume 49, Issue 6, 1983, Pages 1461-1469.

[19] N.H. Rosenbaum, J.C. Owrutsky, L.M. Tack, R.J. Saykally: Velocity modulation laser spectroscopy of negative ions: The infrared spectrum of hydroxide (OH^-), The Journal of Chemical Physics, Volume 84, 1986, Article ID 5308

[20] B.S.D.R. Vamhindi, M. Nsangou, Accurate ab initio potential energy curves and spectroscopic properties of the low-lying electronic states of OH^- and SH^- molecular anions, Molecular Physics, Volume 114, Issue 14, 2016, Pages 2204-2216.

[21] J.A. Smith, P. Jørgensen, Y. Öhrn: A limited basis molecular orbital calculation on H_2O and H_2O^+, The Journal of Chemical Physics, Volume 62, 1975, Article ID 1285

[22] J.E. Reutt, L.S. Wang, Y.T. Lee, D.A. Shirley: Molecular beam photoelectron spectroscopy and femtosecond intramolecular dynamics of H_2O^+ and D_2O^+, The Journal of Chemical Physics, Volume 85, 1986, Article ID 6928

[23] Y.R. Luo: Comprehensive Handbook of Chemical Bond Energies, 1st Edition, 2007, CRC Press, Boca Raton, FL, USA

[24] D.J. Searles, E.I.v. Nagy-Felsobuki: Ab initio variational calculations of molecular vibrational-rotational spectra, 1st Edition, 1993, Springer-Verlag, Berlin, Germany

[25] M. Litorja, B. Ruscic: A photoionization study of the hydroperoxyl radical, HO_2, and hydrogen peroxide, H_2O_2, Journal of Electron Spectroscopy and Related Phenomena, Volume 97, Issue 1-2, 1998, Pages 131-146.

[26] J.B. Burkholder, P.D. Hammer, C.J. Howard: Fourier transform spectroscopy of the ν_2 and ν_3 bands of HO_2, Journal of Molecular Spectroscopy, Volume 151, Issue 2, 1992, Pages 493-512.

[27] E.H. Fink, D.A. Ramsay: High-Resolution Study of the$\tilde{A}^2A' \rightarrow X^2A''$ Transition of HO_2: Analysis of the 000–000 Band, Journal of Molecular Spectroscopy, Volume 185, Issue 2, 1997, Pages 304-324.

[28] S.R. Langhoff, R.L. Jaffe: Theoretical study of the four lowest doublet electronic states of the hydroperoxyl radical: Application to photodissociation, The Journal of Chemical Physics, Volume 71, 1979, Article ID 1475

[29] J.M. Robbe, M. Monnerville, G. Chambaud, P. Rosmus, P.J. Knowles: Theoretical spectroscopic data of the HO_2^+ ion, Chemical Physics, Volume 252, Issue 1-2, 2000, Pages 9-16.

[30] X. Huang, T.J. Lee, A procedure for computing accurate ab initio quartic force fields: Application to HO^+_2 and H_2O, The Journal of Chemical Physics, Volume 129, 2008, Article ID 044312

[31] W.-T. Chan, I.P. Hamilton: The hydroperoxyl anion HO_2^-: Ab initio potential energy surface and vibrational splittings for proton transfer, The Journal of Chemical Physics, Volume 105, Issue 14, 1996, Pages 5907-5914.

[32] R.P. Tuckett, P.A. Freedman, W.J. Jones: The near infra-red emission band of DO_2: determination of the molecular geometry, Molecular Physics, Volume 37, Issue 2, 1979, Pages 403-408.

[33] R.D. Bach, P.Y. Ayala, H.B. Schlegel: A Reassessment of the Bond Dissociation Energies of Peroxides. An ab Initio Study, Journal of the American Chemical Society, Volume 118, Issue 50, 1996, Pages 12758-12765.

[34] J. Hrušák, H. Friedrichs, H. Schwarz, H, Razafinjanahary, H. Chermette: Electron Affinity of Hydrogen Peroxide and the $[H_2,O_2]^{\bullet-}$ Potential Energy Surface. A Comparative DFT and ab Initio Study, The Journal of Physical Chemistry, Volume 100, Issue 1, 1996, Pages 100-110.

[35] P.R. Butler, A.M. Ellis: Application of the Truhlar basis set extrapolation procedure to ab initio calculations on van der Waals complexes, Molecular Physics, Volume 99, Issue 6, 2001, Pages 525-529.

[36] A. Kirrander, M.S. Child, A.V. Stolyarov, Ab initio and quantum-defect calculations for the Rydberg states of ArH, Physical Chemistry Chemical Physics, Volume 8, Issue 2, 2006, Pages 247–255.

[37] M.E. Rosenkrantz, Ab initio study of ArH, ArH^+, Ar_2H, Ar_2H^+, and Ar_4H^+, Chemical Physics Letters, Volume 173, Issue 4, 1990, Pages 378-383.

[38] C.J.H. Schutte: An ab initio molecular orbital study of the argon hydride molecule–ions, ArH^+ and ArD^+, at the MP4(SDQ)/6-311++G(3df,3dp) level. III: a study of some physical properties of ArH^+, compared with those of HeH^+, NeH^+ and KrH^+ and the diatomic Van der Waals molecules He_2, Ne_2, Ar_2 and Kr_2, Chemical Physics Letters, Volume 353, Issue 5-6, 2002, Pages 389-395.

[39] C.J.H. Schutte, An ab initio molecular orbital study of the argon hydride molecule-ions, ArH^+ and ArD^+, at the MP4(SDQ)/6-311++G(3df, 3dp) level. I. The dipole moment, charge distribution, energy levels, internuclear distance and potential energy of the $X^1\Sigma^+$ ground state of the $^{40}Ar^1H^+$ and $^{40}Ar^2D^+$ molecule-ions, Chemical Physics Letters, Volume 345, Issue 5-6, 2001, Pages 525-531.

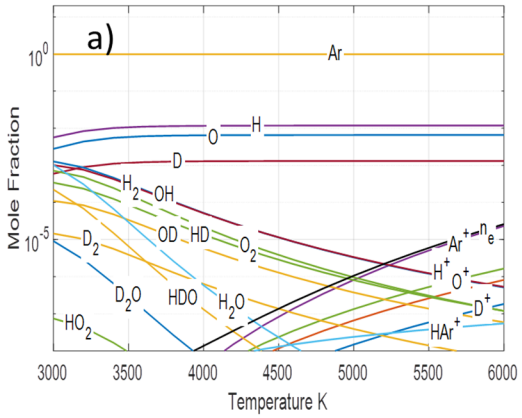

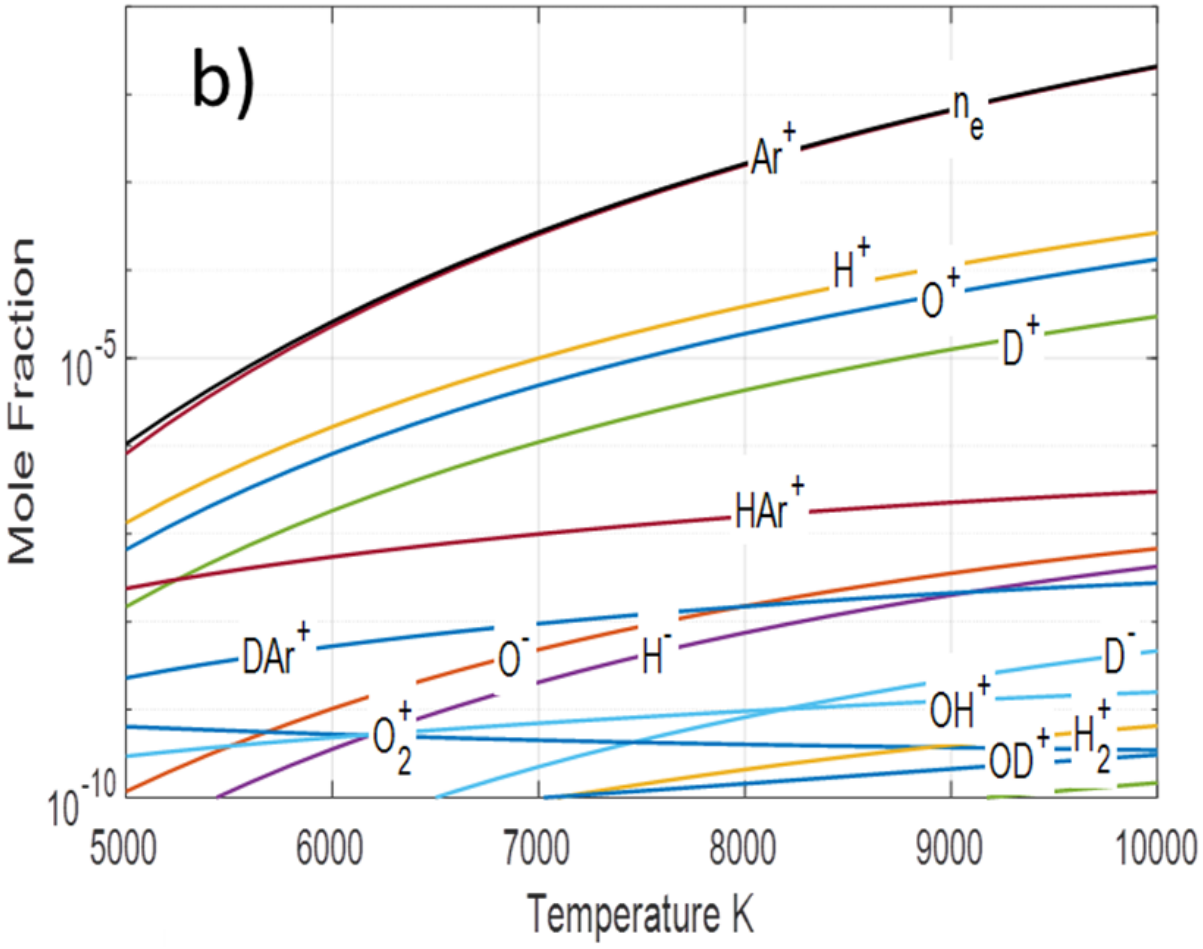
b)
Mole Fraction
10^{-5}
10^{-10}
5000
6000
7000
8000
9000
10000
Temperature K
n_e
Ar^+
H^+
O^+
D^+
HAr^+
DAr^+
O^-
H^-
D^-
OH^+
O_2^+
OD^+
H_2^+

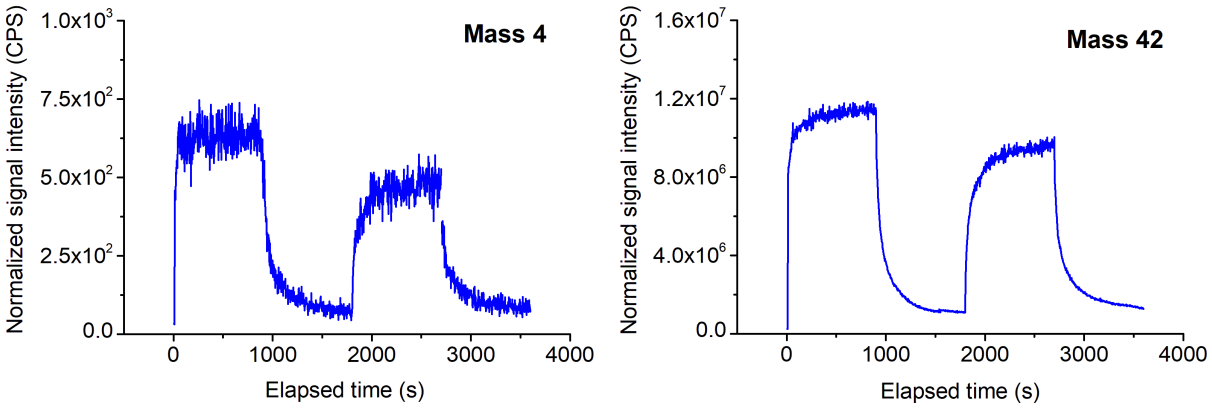

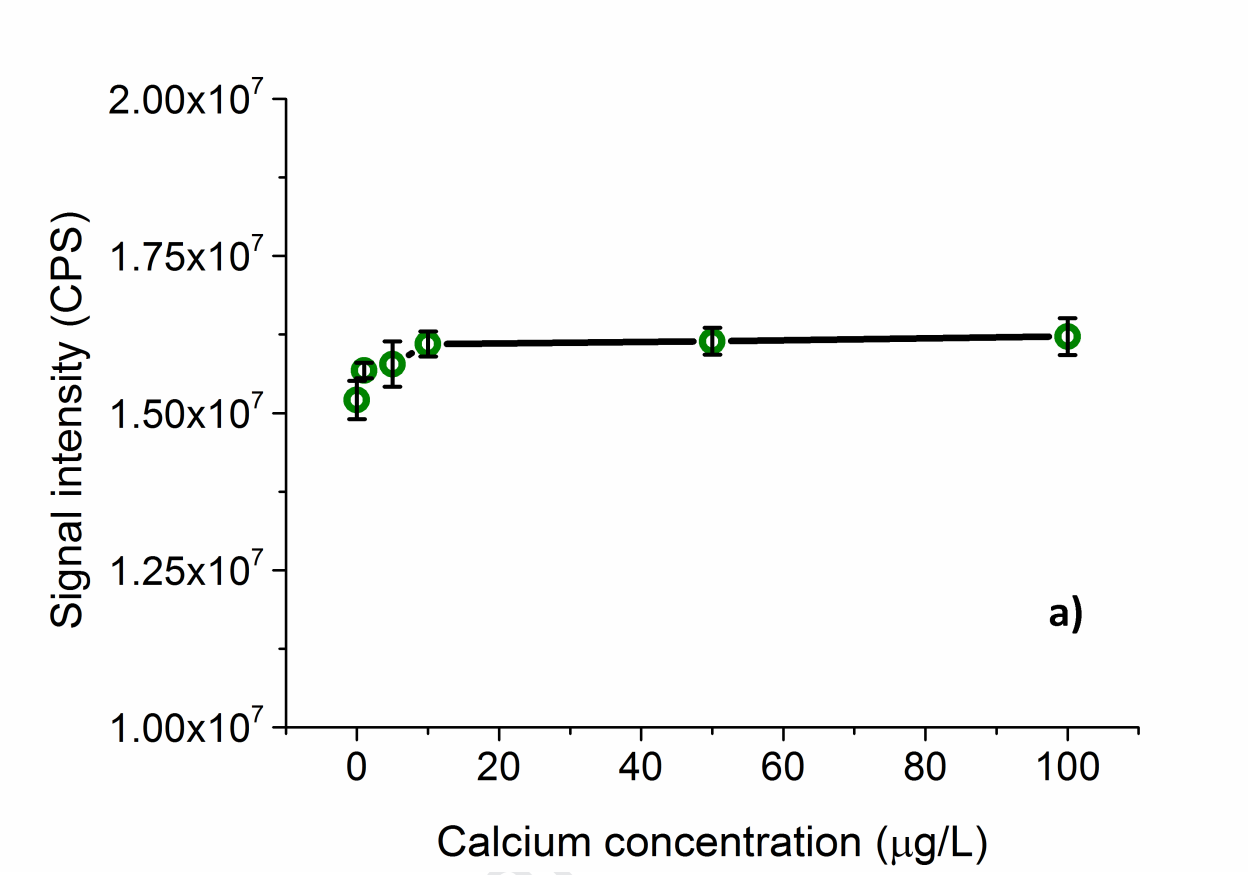
2.00x10^7
1.75x10^7
1.50x10^7
1.25x10^7
1.00x10^7
Signal intensity (CPS)
0
20
40
60
80
100
Calcium concentration (μg/L)
a)

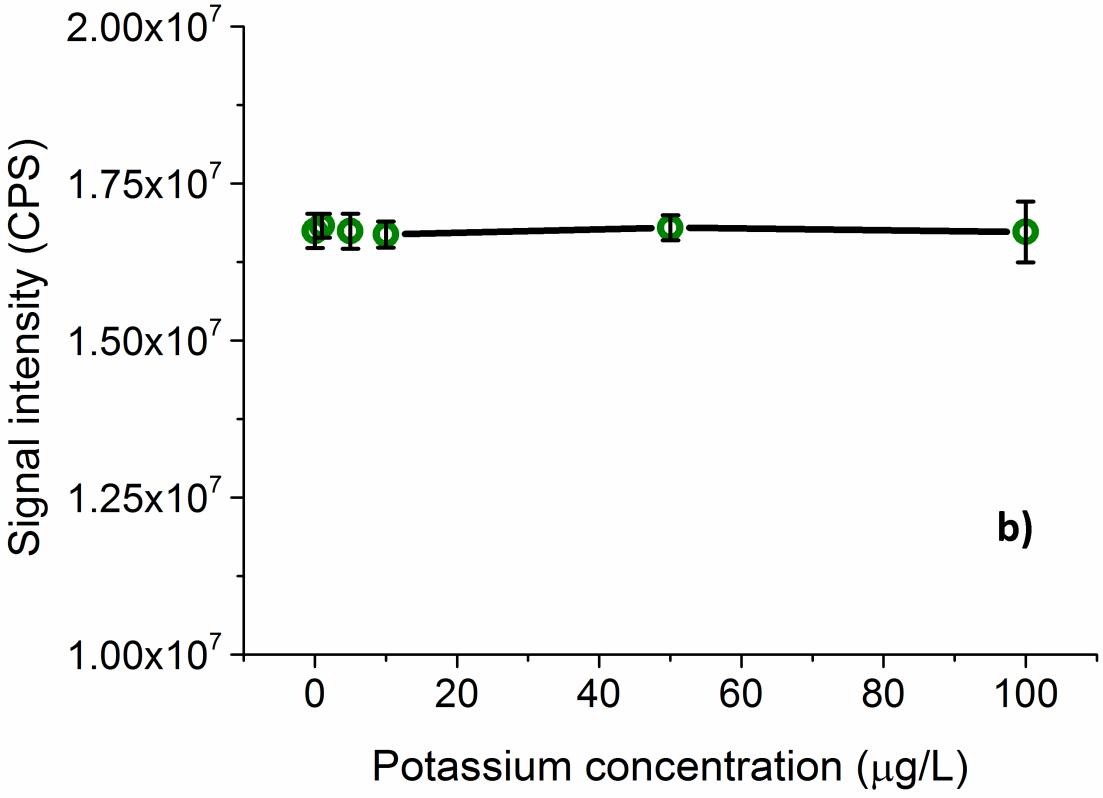
2.00x10^7
1.75x10^7
1.50x10^7
1.25x10^7
1.00x10^7
Signal intensity (CPS)
0
20
40
60
80
100
Potassium concentration (μg/L)
b)

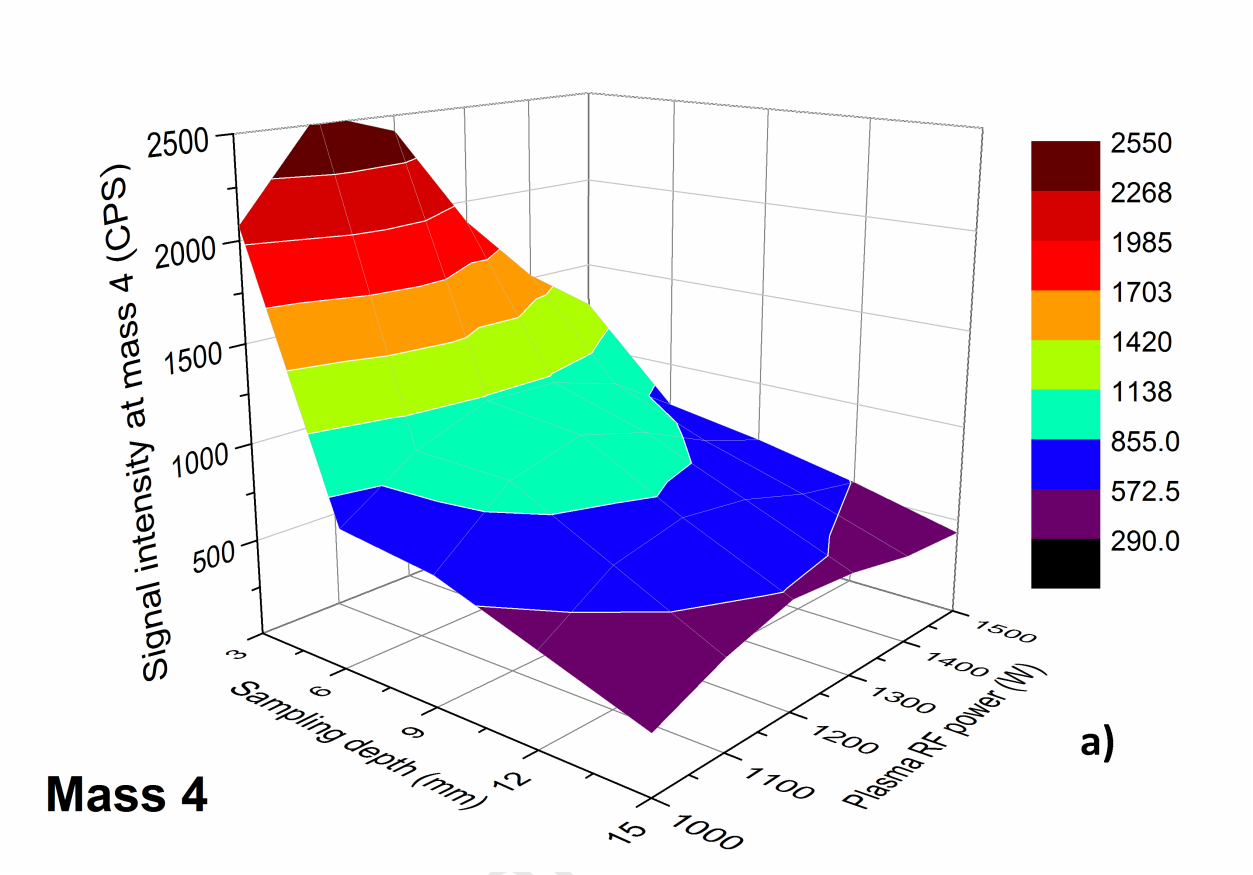
Signal intensity at mass 4 (CPS)
2500
2000
1500
1000
500
Sampling depth (mm)
3
6
9
12
15
Plasma RF power (W)
1000
1100
1200
1300
1400
1500
2550
2268
1985
1703
1420
1138
855.0
572.5
290.0
a)
Mass 4

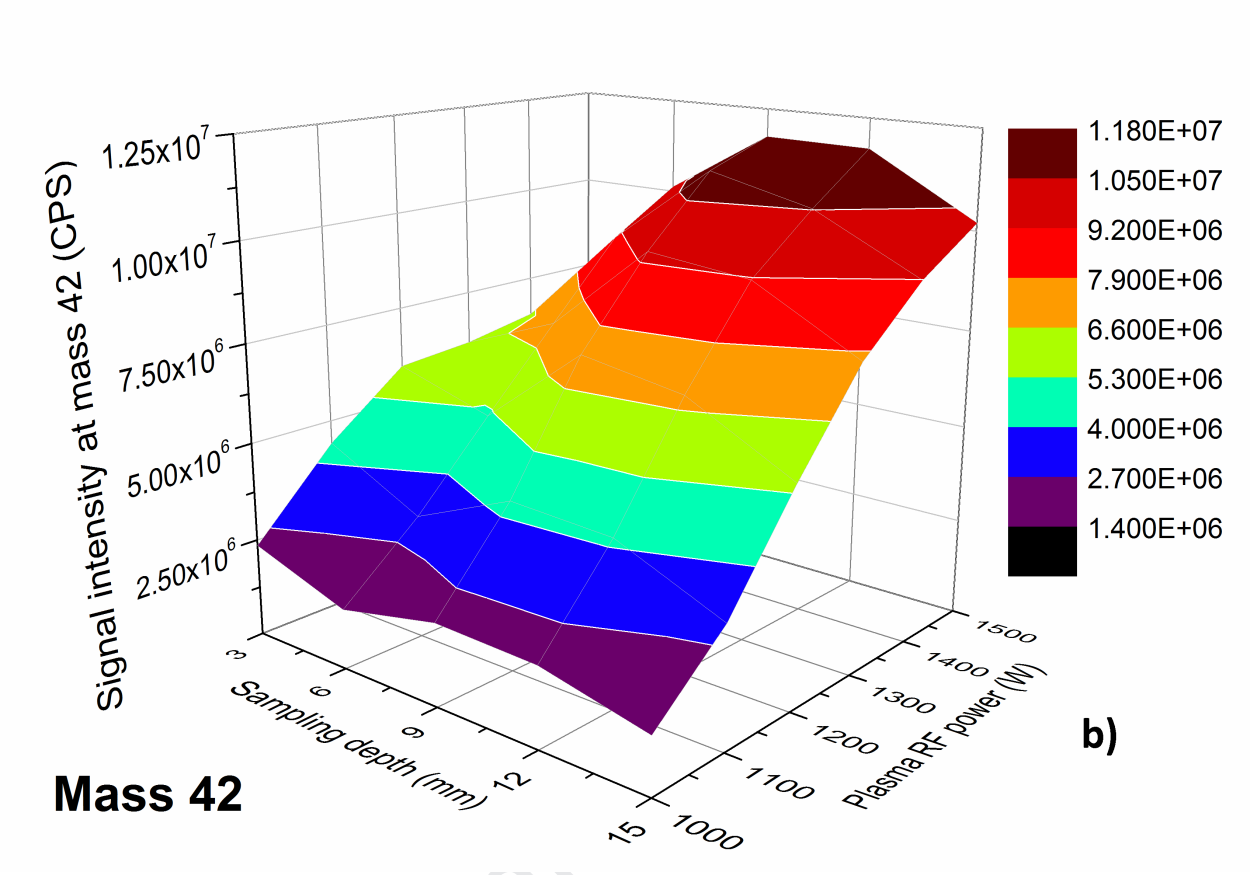
Signal intensity at mass 42 (CPS)
1.25x10^7
1.00x10^7
7.50x10^6
5.00x10^6
2.50x10^6
Sampling depth (mm)
3
6
9
12
15
Plasma RF power (W)
1000
1100
1200
1300
1400
1500
1.180E+07
1.050E+07
9.200E+06
7.900E+06
6.600E+06
5.300E+06
4.000E+06
2.700E+06
1.400E+06
Mass 42
b)

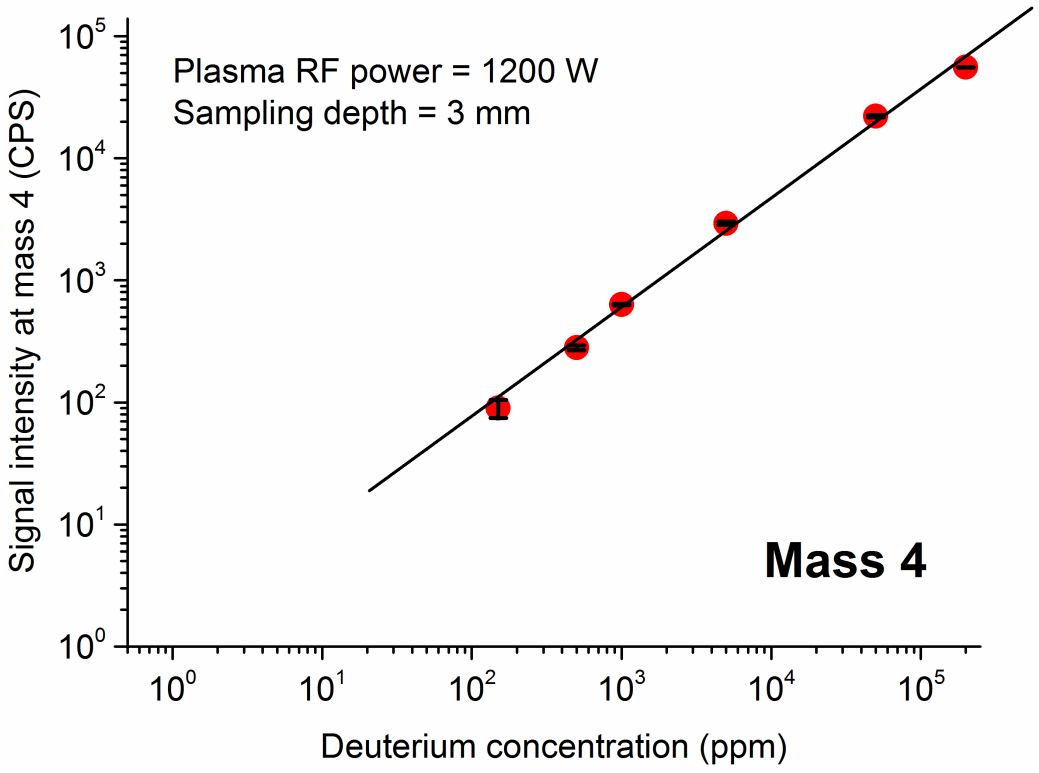
Plasma RF power = 1200 W
Sampling depth = 3 mm
Mass 4
Signal intensity at mass 4 (CPS)
Deuterium concentration (ppm)
10^0
10^1
10^2
10^3
10^4
10^5

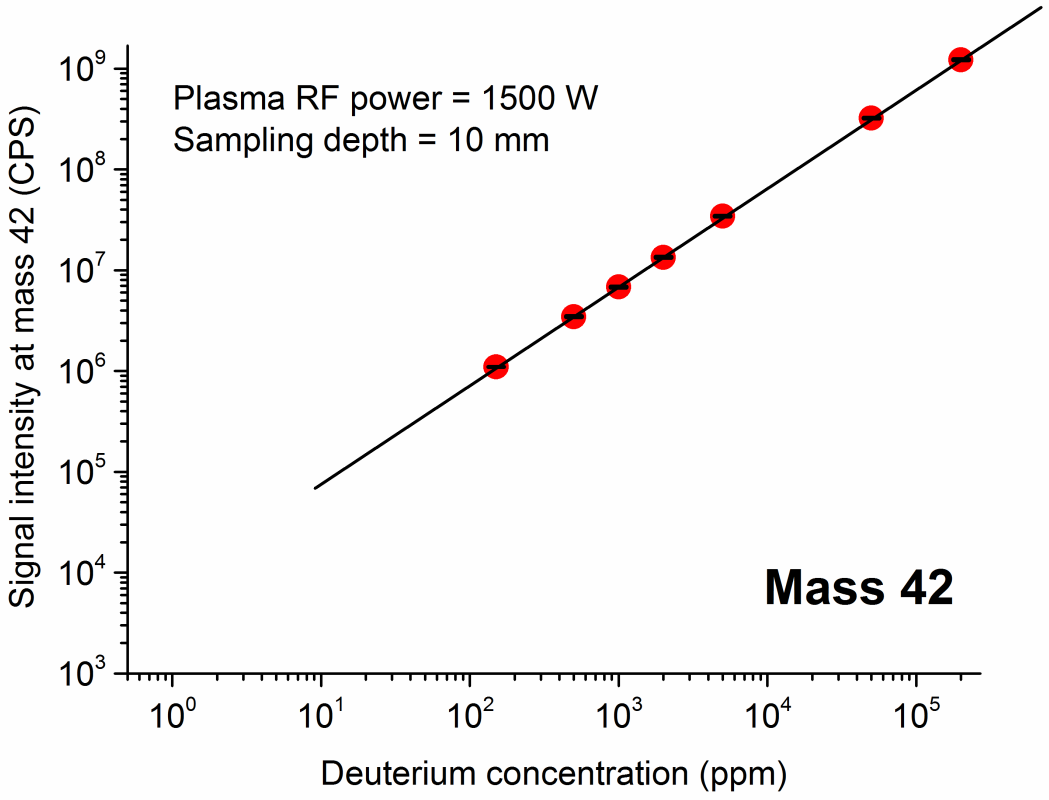
Plasma RF power = 1500 W
Sampling depth = 10 mm
Mass 42
Signal intensity at mass 42 (CPS)
Deuterium concentration (ppm)
10^9
10^8
10^7
10^6
10^5
10^4
10^3
10^0
10^1
10^2
10^3
10^4
10^5

- An equilibrium model was setup to describe the chemical composition of the plasma loaded with heavy water
- Deuterium-containing stable polyatomic species formed in the plasma have been found
- ArD^+ (mass 42) and D_2^+ (mass 4) have been identified as polyatomic species with good analytical potential
- The effect of experimental conditions and interferences on the analytical signals was assessed
- The limit of detection (LOD) was found to be 3 ppm atom fraction for deuterium when measured as ArD (in calcium and potassium free water), or 78 ppm when measured as D_2, with a 4-5 orders of magnitude dynamic range
-

Declaration of interests

☒ The authors declare that they have no known competing financial interests or personal relationships that could have appeared to influence the work reported in this paper.

☐The authors declare the following financial interests/personal relationships which may be considered as potential competing interests:

None

Declaration of interests

☒ The authors declare that they have no known competing financial interests or personal relationships that could have appeared to influence the work reported in this paper.

☐The authors declare the following financial interests/personal relationships which may be considered as potential competing interests:

None